AIAA JOURNAL
Vol. 48, No. 10, October 2010

Beamformed Flow-Acoustic Correlations in a Supersonic Jet

Dimitri Papamoschou*
University of California, Irvine, Irvine, California 92691
and
Philip J. Morris† and Dennis K. McLaughlin‡
Pennsylvania State University, University Park, Pennsylvania 16802

DOI: 10.2514/1.J050325

An experimental study of simultaneous multipoint measurements in the flowfield and acoustic field of a Mach 1.75 cold-air jet is presented. A series of four optical-deflectometer probes measured turbulent fluctuations in or near the jet flow, and eight microphones recorded the far-field pressure in the direction of peak emission. The correlation methodology involves the coherence between the delay-and-sum beamformer outputs of the optical-deflectometer probes and the microphones. This procedure yields results with greater fidelity and higher coherence levels than obtained with individual optical-deflectometer-to-microphone correlations. With the optical-deflectometer probes in the jet shear layer, there is a significant correlation, on the order of 0.1, between the turbulent fluctuations and far-field noise. As the optical-deflectometer probe moves transversely away from the jet, its correlation with the microphone beamformer first drops and then increases. This trend signifies the transition from hydrodynamic to acoustic pressure fields. In the vicinity of the nozzle exit, the peak coherence between the beamformed optical-deflectometer and microphone signals coincides with the physical location of the optical-deflectometer probe. However, as the shear layer thickens downstream, the peak coherence generally lags the probe location, which is a probable result of acoustic refraction by the mean flow.

Nomenclature

D	=	jet diameter
F	=	Fourier transform of f
f	=	signal measured by optical-deflectometer probe
G	=	Fourier transform of g
g	=	delay-and-sum output of microphone beamformer
H	=	Fourier transform of h
h	=	delay-and-sum output of optical-deflectometer beamformer
i	=	$\sqrt{-1}$
M	=	jet Mach number
M_c	=	convective Mach number
P	=	Fourier transform of p
p	=	pressure measured by microphone
S	=	cross spectrum
Sr	=	Strouhal number fD/U
T	=	time delay for optical-deflectometer signals
U	=	jet velocity
U_c	=	convective velocity
$\mathbf{x}, \boldsymbol{\xi}$	=	spatial coordinate vectors
x	=	axial coordinate
y	=	radial coordinate
γ^2	=	coherence
θ	=	polar angle from jet axis
σ^2	=	variance
τ	=	time delay for microphone signals
ω	=	frequency

Presented as Paper 2009-3212 at the 15th AIAA/CEAS Aeroacoustics Conference, Miami, FL, 11–13 May 2009; received 23 November 2009; revision received 4 March 2010; accepted for publication 10 April 2010. Copyright © 2010 by the authors. Published by the American Institute of Aeronautics and Astronautics, Inc., with permission. Copies of this paper may be made for personal or internal use, on condition that the copier pay the $10.00 per-copy fee to the Copyright Clearance Center, Inc., 222 Rosewood Drive, Danvers, MA 01923; include the code 0001-1452/10 and $10.00 in correspondence with the CCC.

*Professor, Department of Mechanical and Aerospace Engineering, 4200 Engineering Gateway; dpapamos@uci.edu. Fellow AIAA.
†Boeing/A. D. Welliver Professor, Department of Aerospace Engineering, 233C Hammond Building; pjm@psu.edu. Fellow AIAA.
‡Professor, Department of Aerospace Engineering, 230A Hammond Building; dkm2@psu.edu. Fellow AIAA.

I. Introduction

THE experimental results presented in this paper represent part of a general effort to understand and model the turbulent noise sources in high-speed jets. Of primary interest is noise in the peak radiation direction that arises from the supersonic motion of large-scale turbulent structures, which have been shown to be modeled well as instability waves [1–6]. The approach involves flow-acoustic correlations using simultaneous multipoint measurements of turbulent fluctuations in the jet and pressure fluctuations in the acoustic far field. This approach can be considered as an extension of the seminal works by Panda et al. [7,8], in which density fluctuations at a single point in the flow were correlated with the signal of a microphone placed in the acoustic far field. Their work showed the high degree of correlation between the large-scale turbulent structures and the far-field noise radiated in the downstream quadrant of supersonic jets.

A natural extension of the past flow-acoustic correlation works is to use multiple simultaneously sampled probes in both the flowfield and acoustic field. Multiple probes (microphones) in the acoustic field allow noise source location using beamforming methods. The use of multiple microphones for noise source location goes back to the polar correlation method by Fisher et al. [9] and the study of phased-array beamforming by Billingsley and Kinns [10]. Since then, phased arrays have found growing application in the detection of airframe noise [11,12] and jet noise [13–15]. Identification of the jet noise source is particularly challenging because it requires modeling of the noise source distribution [9]. One realizes that the only way to accurately detect the jet noise source from far-field measurements is to already know the source! Any number of models thus may fit the far-field observations. To make tangible progress, the far-field measurements must be accompanied by turbulence measurements in the flow. These measurements provide additional information that may aid in the construction of physically meaningful models for the noise source. Relevant quantities are the eddy correlation length scales and the eddy convective velocities. Both require the simultaneous measurement of turbulent fluctuations using at least two probes or one probe and a reference signal. Such measurements are so challenging in high-speed jets that for about 20 years the hot-wire measurements of Troutt and McLaughlin [2] were the only ones in supersonic jets that produced continuous time signals and convection velocity measurement capability. This was

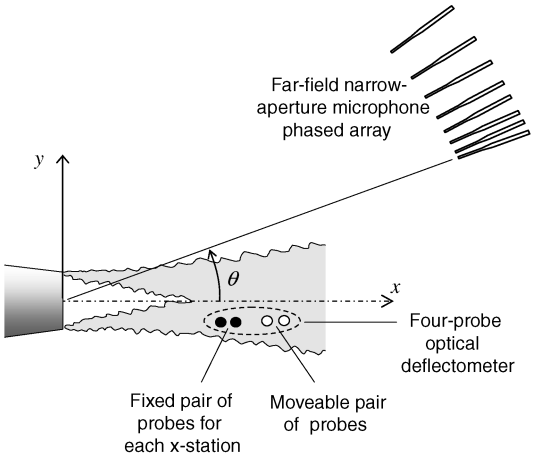

Fig. 1 Schematic of OD and microphone array setup.

accomplished by measuring in a low-pressure environment that also resulted in reduced Reynolds numbers.

Advances in high-speed flowfield instrumentation developed in the last 10 years have opened new opportunities for experimentalists.

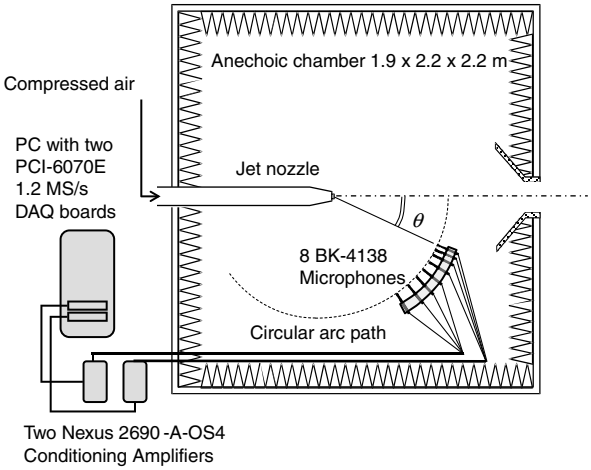

Fig. 2 Jet aeroacoustics measurement.

The recent particle image velocimetry (PIV) measurements in compressible heated jets by Bridges [16] have been able to obtain space–time velocity correlation data for a limited number of high-speed jets. Within the same NASA organization, Panda and Seasholtz [8] have developed a unique Rayleigh scattering instrumentation system for the measurement of density and velocity fluctuations. In their most recent work, Panda et al. [7] have used their Rayleigh scattering instrument to measure correlations between velocity fluctuations in the jet and signals of microphones placed in the acoustic far field. These data have shown the high degree of correlation between the large-scale turbulent structures and the far-field noise radiated in the downstream quadrant of supersonic jets. Hileman et al. [17] used a combination of microphone beamforming (done mostly in the time domain) and flow visualization to study the connection between highly energetic turbulence and noise events in high-speed jets; our study shares some similarities with their approach. Finally, application of the optical-deflectometer (OD) to high-speed jets by Doty and McLaughlin [18,19] and Petitjean et al. [20] has produced extensive data on two point space–time correlations that cover a substantial spatial extent of jets over a wide range of Mach numbers. Although this instrument measures correlations in density gradients in the flow, it has been shown [19] that such data measured in high-speed (subsonic) jets are equivalent to velocity fluctuation correlation data measured by a number of prior investigators in low-speed jet flows. In addition, comparisons of the OD data with other recently developed techniques has demonstrated the equivalence of the correlation data in supersonic jets. (An example of such comparisons is presented in the Results section.) It is this OD technique that is applied here for multiple-probe measurements in the flow.

This paper provides an initial framework for combining simultaneous multipoint measurements in the flow and the acoustic far field into a method for the characterization the jet noise sources. The approach is based on beamforming both the microphones and the flow probe signals, then cross-correlating the two beamformed outputs. The overall approach is illustrated in Fig. 1. Initial results for an unheated Mach 1.75 jet are reported in the present paper.

II. Experimental Setup

The experiments at the University of California, Irvine (U. C. Irvine) were performed on perfectly expanded round jets of Mach numbers 0.9, 1.5, and 1.75. The supersonic jets were unheated and the subsonic jet was operated at a simulated heated condition (using helium–air mixtures) so that its velocity matched the velocity of the

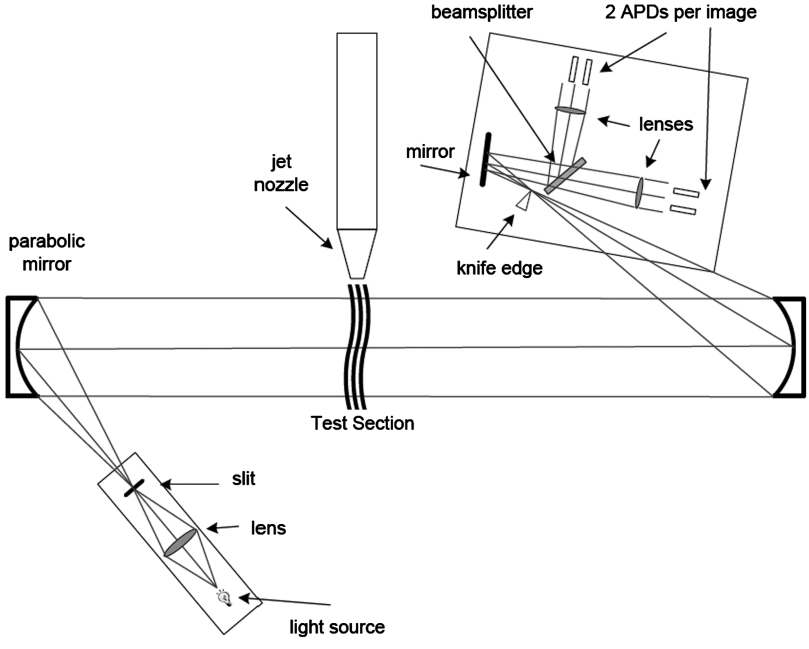

Fig. 3 Basic design of optical deflectometer.

$M = 1.5$ unheated jet. Here, results for the $M = 1.75$ jet with velocity $U = 474$ m/s and estimated convective Mach number $M_c = 1.1$ are reported. The jet was produced by a 12.7 mm nozzle designed by the method of characteristics. The nozzle was supplied by unheated air at a nozzle pressure ratio of 5.3, resulting in a perfectly expanded flow. The jet Reynolds number was 670,000.

Noise measurements were performed in the aeroacoustic facility shown in Fig. 2. A microphone array consisted of eight 3.2 mm condenser microphones (Bruel & Kjaer, model 4138) arranged on a circular arc centered in the vicinity of the nozzle exit. The polar aperture of the array was 30° and the array radius was 1 m. The angular spacing of the microphones was logarithmic. The entire array structure was rotated around its center to place the array at the desired polar angle. The microphones were connected, in groups of four, to two amplifier/signal conditioners (Bruel & Kjaer, Nexus 2690-A-OS4) with a high-pass filter set at 300 Hz and a low-pass filter set at 100 kHz.

The basic operation of the optical deflectometer is illustrated in Fig. 3. The present setup used four probes, two stationary and two moveable (Fig. 1), with four avalanche photodiodes. This is a new system that was designed, fabricated and tested at Pennsylvania State University before being shipped to U. C. Irvine for operation. A detailed description of the system can be found in Veltin et al. [21].

The eight microphone signals and four optical-deflectometer outputs (12 channels total) were sampled simultaneously at 160 kHz by two multifunction data acquisition boards (National Instruments PCI-6070E) installed in a Pentium 4 personal computer. The maximum resolved frequency was thus 80 kHz. National Instruments LabVIEW software was used to acquire the signals.

III. Correlation Methodology

A. Correlation Between an Individual OD Probe and a Beamformed Microphone Array (OD-DAS$_{\mathbf{mic}}$)

The correlation between the OD signal with the output of the focused array is illustrated in Fig. 4. The purpose of these experiments is to investigate correlations between the deflectometer signal and the far-field pressure signal emanating from the vicinity of the probe volume of the deflectometer. To focus the array at a certain point $\boldsymbol{\xi}$, the common delay-and-sum (DAS) method is used:

$$g(\boldsymbol{\xi}, t) = \sum_{m=1}^{M} p_m(t + \tau_m(\boldsymbol{\xi})) \tag{1}$$

with $p_m(t)$ the signal of microphone m and $\tau_m(\boldsymbol{\xi})$ the acoustic propagation time from point $\boldsymbol{\xi}$ to microphone m. The time delay is based on a straight path between focus point $\boldsymbol{\xi}$ and microphone m. The OD probe is located at point $\mathbf{x}$ and measures the signal $f(\mathbf{x}, t)$. The cross spectrum of the OD and DAS$_{\text{mic}}$ signals is given by

$$S_{fg}(\mathbf{x}, \boldsymbol{\xi}, \omega) = \langle F(\mathbf{x}, \omega) G^*(\boldsymbol{\xi}, \omega) \rangle \tag{2}$$

where F and G are the Fourier transforms of f and g, respectively, and * signifies the complex conjugate. From Eq. (1), the Fourier transform of the DAS$_{\text{mic}}$ signal is

$$G(\boldsymbol{\xi}, \omega) = \sum_{m=1}^{M} P_m(\omega) e^{i\omega\tau_m(\boldsymbol{\xi})} \tag{3}$$

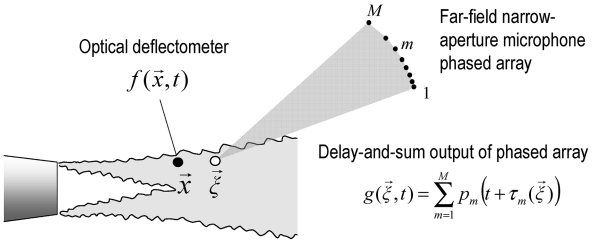

Fig. 4 Illustration of the correlation of the OD signal with the DAS output of the microphone array.

where P_m is the Fourier transform of p_m. Substitution into Eq. (2) gives

$$S_{fg}(\mathbf{x}, \boldsymbol{\xi}, \omega) = \sum_{m=1}^{M} \langle F(\mathbf{x}, \omega) P_m^*(\omega) \rangle e^{-i\omega\tau_m(\boldsymbol{\xi})} \tag{4}$$

To understand the correlations between flow and acoustics, it is important to present this cross spectrum in the nondimensional form of coherence. To do this, we first compute the autospectrum of the OD signal

$$S_{ff}(\mathbf{x}, \omega) = \langle F(\mathbf{x}, \omega) F^*(\mathbf{x}, \omega) \rangle \tag{5}$$

and the autospectrum of the DAS signal, often referred to as the array beamformer output,

$$\begin{aligned} S_{gg}(\boldsymbol{\xi}, \omega) &= \langle G_n(\boldsymbol{\xi}, \omega) G_m^*(\boldsymbol{\xi}, \omega) \rangle \\ &= \sum_{m=1}^{M} \sum_{n=1}^{M} \langle P_n(\omega) P_m^*(\omega) \rangle e^{i\omega[\tau_n(\boldsymbol{\xi}) - \tau_m(\boldsymbol{\xi})]} \end{aligned} \tag{6}$$

Now the coherence of the OD-DAS$_{\text{mic}}$ signals is defined as follows:

$$\gamma_{fg}^2(\mathbf{x}, \boldsymbol{\xi}, \omega) = \frac{|S_{fg}(\mathbf{x}, \boldsymbol{\xi}, \omega)|^2}{S_{ff}(\mathbf{x}, \omega) S_{gg}(\boldsymbol{\xi}, \omega)} \tag{7}$$

In this paper results for the OD-DAS$_{\text{mic}}$ cross spectra with the OD probe at various points inside and outside the $M = 1.75$ jet are presented.

B. Correlation Between Beamformed OD Signals and Beamformed Microphone Array (DAS$_{\mathbf{OD}}$-DAS$_{\mathbf{mic}}$)

To construct a single signal out of the four OD probes (when they are aligned in the axial direction), a delay-and-sum method is used. This involves time delays based on the convective velocity U_c. The convective velocity can be determined using space–time correlations of the OD probe signals or, as will be shown below, by maximizing the value of the delay-and-sum variance. Consider the axial arrangement of Fig. 5. The OD probes are at positions $x + \Delta x_j$, with $\Delta x_1 = 0$. Time and space are referenced to the position x of the first probe. The delay-and-sum beamformer for the optical deflectometer (DAS$_{\text{od}}$) is

$$h(x, t) = \sum_{j=1}^{J} f_j(x, t + T_j), \qquad T_j = \frac{\Delta x_j}{U_c} \tag{8}$$

where J is the total number of probes (in this case $J = 4$). Before discussing the spectrum of $h(x, t)$, it is important to realize an important property of its variance:

$$\sigma_h^2(x) = \langle h(x, t) h(x, t) \rangle = \sum_{i=1}^{J} \sum_{j=1}^{J} \langle f_i(x, t + T_i) f_j(x, t + T_j) \rangle \tag{9}$$

The summation is made up of variances of the individual probe signals, which are constants, and cross-correlations between probe signals. The latter are in fact space–time correlations, maximized when $T_j = \Delta x_j / U_c$. Therefore, maximization of σ_h^2 offers an alternative means to determine the convective velocity U_c.

Consider the cross spectrum of the DAS$_{\text{mic}}$ and DAS$_{\text{od}}$ signals, given, respectively, by Eqs. (1) and (8). It is assumed that the OD probes and the beamformer focus of the microphone array fall on the same axial line (in this experiment the nozzle centerline or lip line), so the vector notation is omitted from the beamforming point. The DAS$_{\text{mic}}$-DAS$_{\text{od}}$ cross spectrum is

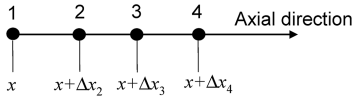

Fig. 5 Sequence of OD probes used in OD beamforming.

$$S_{hg}(x,\xi,\omega) = \langle H(x,\omega)G^*(\xi,\omega)\rangle \tag{10}$$

From Eq. (8), the Fourier transform of the $\mathrm{DAS}_{\mathrm{od}}$ signal is

$$H(x,\omega) = \sum_{j=1}^{J} F_j(x,\omega)e^{i\omega T_j} \tag{11}$$

Substitution of Eqs. (3) and (11) in Eq. (10) yields

$$S_{hg}(x,\xi,\omega) = \sum_{j=1}^{J}\sum_{m=1}^{M}\langle F_j(x,\omega)P_m^*(\omega)\rangle e^{i\omega[T_j-\tau_m(\xi)]} \tag{12}$$

Using steps similar to those for deriving the autospectrum of the $\mathrm{DAS}_{\mathrm{mic}}$ signal, Eq. (6), the autospectrum of the $\mathrm{DAS}_{\mathrm{od}}$ signal is

$$\begin{aligned} S_{hh}(x,\omega) &= \langle H(x,\omega)H^*(x,\omega)\rangle \\ &= \sum_{j=1}^{J}\sum_{i=1}^{J}\langle F_j(x,\omega)F_i^*(x,\omega)\rangle e^{i\omega(T_j-T_i)} \end{aligned} \tag{13}$$

The coherence of the $\mathrm{DAS}_{\mathrm{od}}$-$\mathrm{DAS}_{\mathrm{mic}}$ signals is

$$\gamma_{hg}^2(x,\xi,\omega) = \frac{|S_{hg}(x,\xi,\omega)|^2}{S_{hh}(x,\omega)S_{gg}(\xi,\omega)} \tag{14}$$

Using Parseval's theorem the variance of the $\mathrm{DAS}_{\mathrm{od}}$ signal can be evaluated using the autospectrum of Eq. (13); that is,

$$\sigma_h^2(x) = \int_0^\infty S_{hh}(x,\omega)\,\mathrm{d}\omega \tag{15}$$

Therefore the convective velocity can be determined by maximizing the integral of Eq. (15). The result is then used in Eq. (8) to determine the time delays T_j of for the optical-deflectometer beamforming. In Eq. (12), the axial position x (chosen here as the location of the first probe) represents the position of the OD array as a whole. Selecting another probe as the reference probe amounts to a uniform time shift for all the Δt_j, which changes the phase of the cross spectrum $S_{hg}(x,\xi,\omega)$ but not its magnitude. Hence the coherence given by Eq. (14) is invariant to the selection of the reference probe.

IV. Results

For all the results shown, the microphones were located in the aft quadrant at polar angles ranging from 23.7 to 53.5 deg, as shown in Fig. 6. The OD probes translated axially and normally in the jet and its vicinity. Since the OD sensing volume includes an integration through the unsteady flow there is some uncertainty in this effect on the measurements. To address this, comparisons have been made

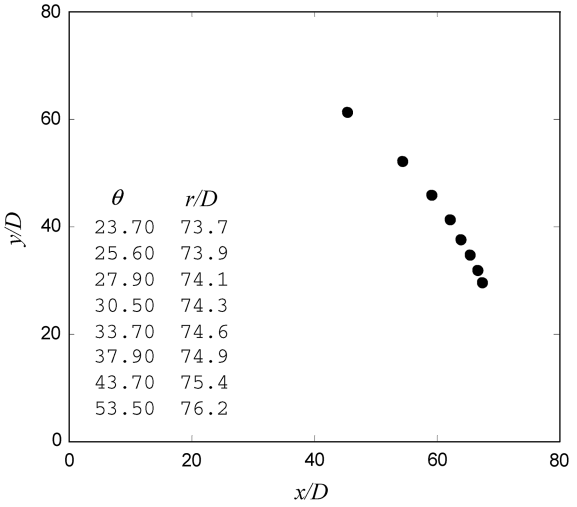

Fig. 6 Microphone positions.

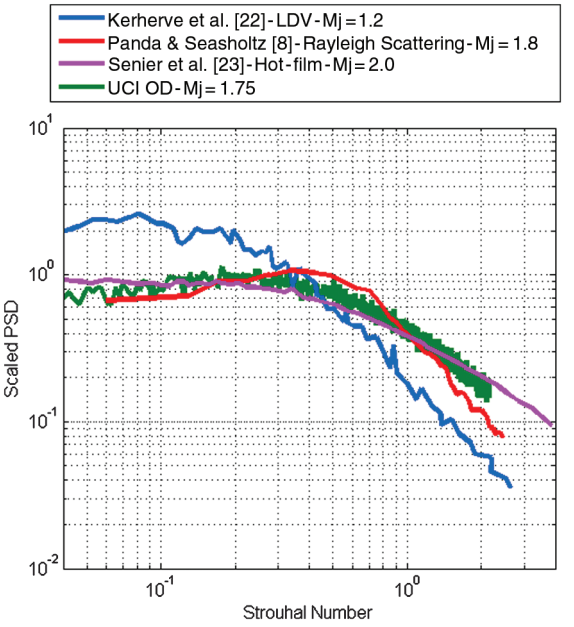

Fig. 7 Comparison of optical-deflectometer spectra with those from three other techniques.

with all readily available turbulence spectral data taken by other researchers in supersonic round jet flows. A summary of such spectra is presented in Fig. 7 in which the present OD data are compared with data from a laser Doppler velocimeter [22], a wedge hot-film probe [23] and a Rayleigh scattering density measurement system [7]. The spectra have been normalized with their mean square values. All the normalized spectra in this figure were recorded on the lip line of a supersonic cold jet at $x/D = 6$. It is noted that the three spectra measured between $M = 1.75$ and $M = 2.0$ agree very closely across all the measured frequencies, despite the significant difference in the measurements systems. The laser Doppler anemometry data measured by Kerherve et al. [22] depart significantly from the other data. But comparisons of the lower Mach number measurements have been shown to be in close agreement with subsonic jet measurements performed recently by Morris and Zaman [24]. The data shown in Fig. 7 provide substantial validation for the use of the optical deflectometer for supersonic jet turbulence measurements. More extensive comparisons and explanation are given by Day [25].

Moving to the microphone measurements, the first data to be shown are the microphone beamformer map for the $M = 1.75$ jet. Figure 8 plots isocontours of the $\mathrm{DAS}_{\mathrm{mic}}$ autospectrum S_{gg} [Eq. (6)] on the $x/D - Sr$ plane, where $Sr = fD/U$ is the Strouhal number of the jet. The map shows a global peak at $x/D = 12$ and $Sr = 0.15$. As

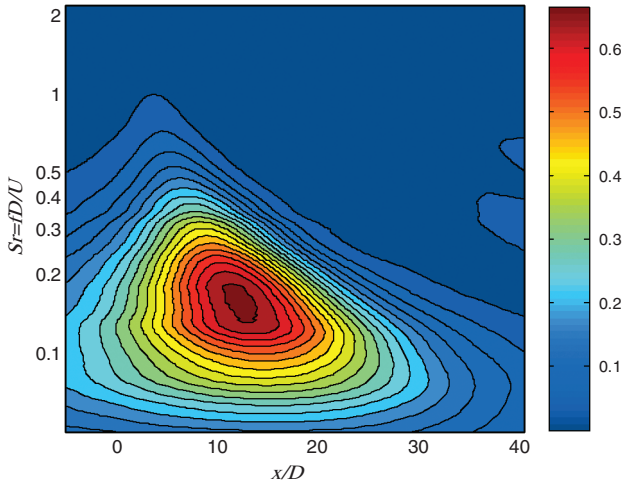

Fig. 8 Delay-and-sum beamform map of $M = 1.75$ jet with microphones as shown in Fig. 6.

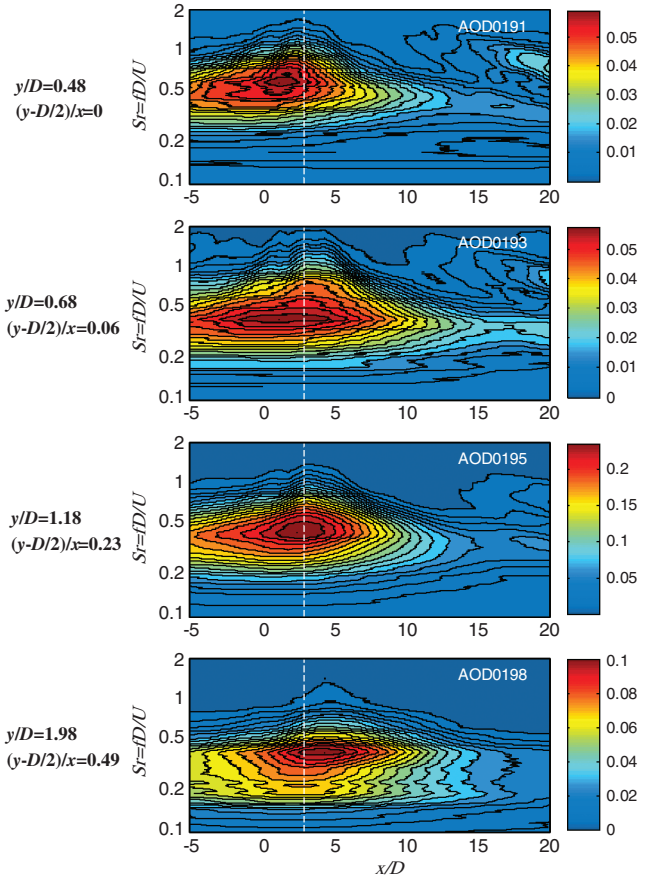

Fig. 9 Isocontours of coherence between single OD probe at $x/D = 3.0$ and delay-and-sum output of microphone array $\mathrm{DAS_{mic}}$. Dashed white line in this and following coherence plots shows the axial location of the probe.

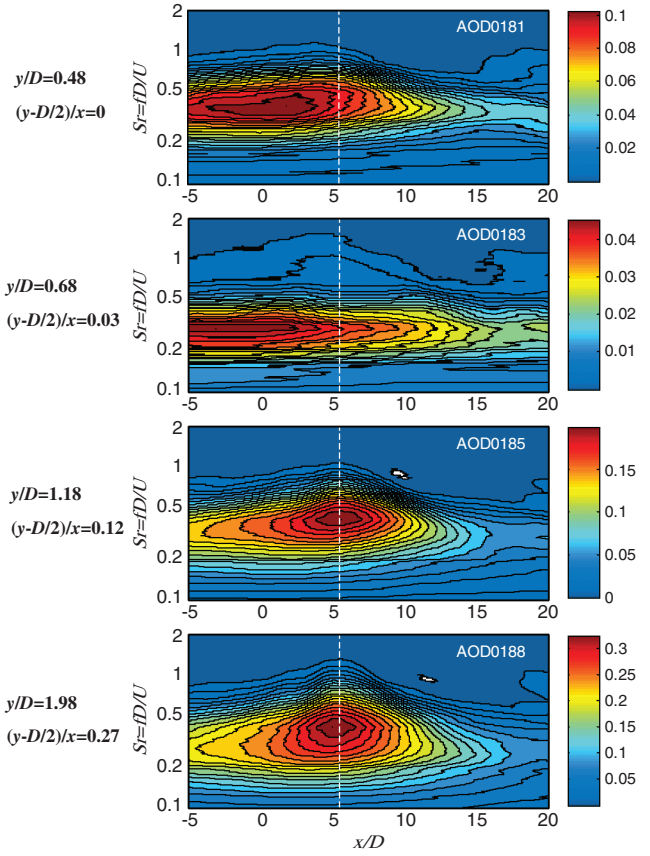

Fig. 10 Isocontours of coherence between single OD probe at $x/D = 5.5$ and delay-and-sum output of microphone array $\mathrm{DAS_{mic}}$.

the Strouhal number increases, the peak intensity moves toward the nozzle exit, which is a result consistent with many previous studies.

Now the OD-$\mathrm{DAS_{mic}}$ coherence results in the form of contour plots on the $x/D - Sr$ plane are presented. A dashed white line indicates the axial position of the reference OD probe. The same format will be used for all the coherence plots. First, consider the evolution of the OD-$\mathrm{DAS_{mic}}$ coherence as the OD probe moves transversely from the jet lip line to a position outside the jet flow. Figure 9 shows this evolution for the OD probe at $x/D = 3.0$ for four radial positions of the OD. Also shown in the figure, below the transverse distance, is the probe location in terms of a similarity coordinate $(y - D/2)/x$. This provides an indication of the relative location of the probes in the jet shear layer as the downstream distance changes. For reference, at $(y - D/2)/x = 0.1$, the axial turbulence intensity has fallen to 50% of its maximum value near $(y - D/2)/x = 0$ (see Davies [26]). With the OD probe close to the lip line ($y/D = 0.48$), a peak coherence of 0.06 is measured. This peak occurs about two jet diameters upstream of the probe location and at Strouhal number $Sr = 0.6$. One might suspect calibration errors for the mismatch between the coherence peak location and the probe locations, but, as discussed below, this is not the case. As the OD probe moves outside the jet flow, the coherence strengthens and its peak location moves toward the probe location. At $y/D = 1.18$, the coherence peaks at 0.25. Further movement of the probe outside the jet leads to a smaller coherence as the probe moves outside the region of peak noise emission. It is notable that, with the OD probe outside the jet, the peak coherence occurs exactly at the axial location of the OD probe. This indicates that the microphone array is properly aligned and calibrated, and that the spatial lag seen in Fig. 9 is connected to refraction of the sound waves by the mean jet flowfield. As shown by Bogey and Bailly [27], the ray path connecting a point inside the jet to a point outside the jet is not a straight line; rather, it is bent inside the jet because of the gradients of mean velocity and speed of sound. As a result, the time delay $\tau_m(\boldsymbol{\xi})$ used in the beamforming [Eq. (1)] is different from that calculated using a straight ray path. This can cause a shifting of the focus from its intended position, as well as blurring of the focal point.

Similar phenomena are observed with the OD probe located at $x/D = 5.5$ and 8.0, shown, respectively, in Figs. 10 and 11. One interesting feature that is more evident in these figures is the variation in the maximum coherence as the OD probe is moved outward from the lip line. Initially there is a decrease in the maximum coherence and then an increase to higher levels than obtained with the OD probe on the lip line. Though the reason for this behavior is not fully understood, an explanation can be found in the response of the OD. The OD senses fluctuations in the density gradient. These can be caused by velocity fluctuations that perturb the mean density gradient or by pressure fluctuations. On the jet lip line the velocity fluctuations are at their maximum and are probably the dominant cause of the fluctuations detected by the OD. In turn, these velocity fluctuations are dominated by the motions of the large-scale turbulent structures, which are known to correlate well with the noise radiation in the peak noise direction in high-speed jets. Moving outward from the jet lip line the velocity fluctuations decrease and initially the hydrodynamic pressure fluctuations will control the OD signal. Since only a small fraction of the hydrodynamic pressure fluctuations radiate as sound the correlation with the far-field pressure is likely to decrease. Further out from the jet lip line, well outside the edge of the jet, the OD senses the acoustic fluctuations, which are clearly well correlated with the far-field sound. This explains the eventual increase in the coherence levels. A number of studies have examined the transition between the hydrodynamic and acoustic fields in the vicinity of the shear layer of turbulent jets [28–30]. Transition criteria for the transverse distance y have been proposed [29,30], the most comprehensive of which appears to be that of Guitton et al. [30], $ky/M_a = 4.3(M_a/0.3)^{-0.375}$, with k the wave number and M_a the acoustic Mach number. For our jet this translates to $y/D = 0.78/Sr$. Referring to the $\mathrm{DAS_{mic}}$-OD

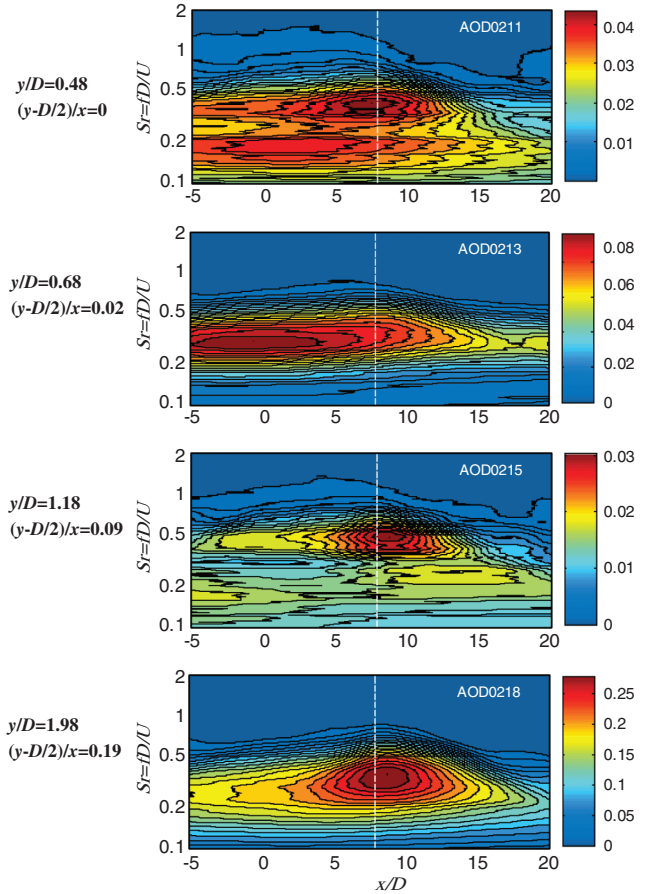

Fig. 11 Isocontours of coherence between single OD probe at $x/D = 8.0$ and delay-and-sum output of microphone array DAS_{mic}.

correlations of Figs. 8 and 9, for $Sr \approx 0.4$ (where the peak occurs), the corresponding transition value is $y/D = 1.9$, which is consistent with the y/D values where the coherence is observed to increase.

The clear advantage of the processing used in Figs. 9–11 is seen by comparing the plots with similar OD to microphone correlations performed without use of the beamformer. Figure 12, taken from Veltin et al. [21], displays isocontours of the coherence of the single OD probe traversed along the lip line of the jet correlated with a single microphone located at the approximate center of the micro-

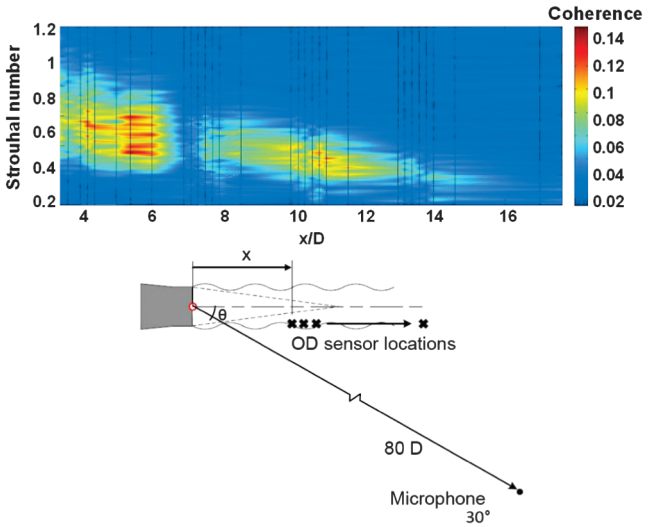

Fig. 12 Isocontour plots of the coherence between an OD sensor scanning along the lip line of the jet and a microphone fixed in the far-field at $\theta = 30°$ [21].

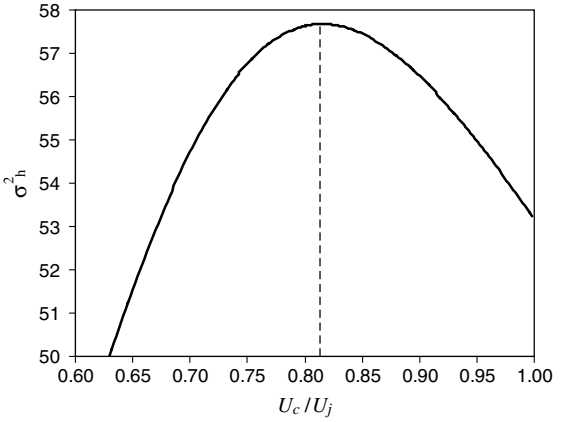

Fig. 13 Determination of convective velocity U_c by maximization of the variance σ_h^2 of the delay-and-sum output of the optical deflectometer.

phone array. The resulting fidelity has nowhere near the clarity seen in the corresponding isocontours of the coherence of the OD and the beamformed microphone array output (shown in the top part of Fig. 9). The simpler processing used in Fig. 12 does produce some additional insights, but not with the same clarity that is evident in the results of Figs. 9–11 of the present paper.

Moving now to the DAS_{od}-DAS_{mic} correlations, Fig. 13 shows an example of the determination of U_c by maximizing the variance of the OD beamformer, as discussed in Sec. III.B. Figures 14–17 show DAS_{od}-DAS_{mic} coherences for various OD probe locations and compare them to the OD-DAS_{mic} coherences at the same reference probe location. For each case, the DAS_{od} is based on the convective velocity determined by maximization of the DAS_{od} variance, Eq. (10). In Fig. 14, the reference OD probe is located on the lip line near the nozzle exit at $x/D = 2.0$. Near the nozzle exit, the shear layer thickness is too small to cause significant bending of the rays emanating from the probe location. As a result, the peaks of the coherences coincide with the probe location. The DAS_{od}-DAS_{mic} coherence peaks at 0.12 and the OD-DAS_{mic} coherence peaks at 0.05. Therefore, the OD beamforming enhances significantly the correlations with the microphone array. As the reference OD probe moves downstream along the lip line to $x/D = 3.5$, Fig. 15, the shear layer thickens and refraction effects become more pronounced. As a result, the coherences peak about one jet diameter upstream of the reference OD probe location. The DAS_{od}-DAS_{mic} coherence is again about twice as strong as the OD-DAS_{mic} coherence. Further downstream on the lip line, at $x/D = 10$ (Fig. 16), the refraction effects cause significant blurring of the coherence peak, but again the enhanced coherence of DAS_{od}-DAS_{mic} can be observed The doubling of the maximum coherence when the beamformed OD signal is used emphasizes the fact that the acoustic radiation in the peak noise direction is associated with turbulent structures that propagate at U_c and, perhaps more important, are correlated over the relatively large axial separation of the OD sensors. This is strong evidence that the noise is dominated by coherent large-scale turbulent structures.

When the reference probe is moved to the centerline of the jet at $x/D = 10$, Fig. 17, the coherence peaks move near the nozzle exit and the coherence pattern is severely smeared. This is believed to be due to the severe distortion of the ray paths emanating from a point on the centerline of the jet. This is a major effect that impacts the ability to accurately image noise sources. It underscores the need to account for refraction effects in noise source imaging methods. In addition, it should be noted that when the OD probe is interrogating the jet centerline the light beam will be influenced by fluctuations at all locations across the jet. This reflects the integration effect of the schlieren system. Examination of the plots in Figs. 14–17 shows the reduction of the peak Strouhal number with axial distance, from $Sr \approx 0.6$ at $x/D = 2.0$ to $Sr \approx 0.25$ at $x/D = 10$. This trend is consistent with the evolution of peak noise with axial distance seen in the beamformer output of Fig. 8.

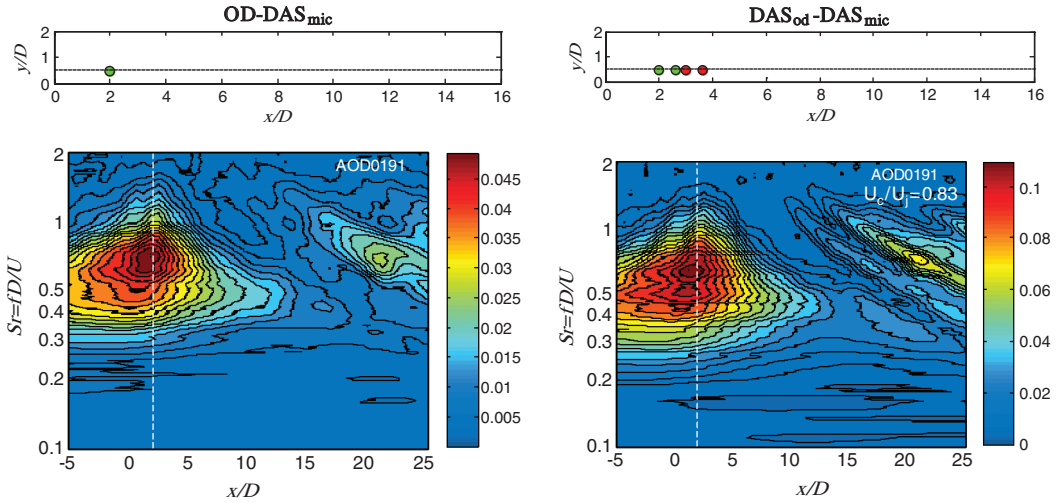

Fig. 14 Isocontours of coherence for OD-DAS$_{mic}$ and DAS$_{od}$-DAS$_{mic}$. Reference probe at $x/D = 2.0$ and $r/D = 0.48$ (lip line). Computed convective velocity $U_c = 0.83\ U_j$ was used in DAS$_{od}$ beamforming.

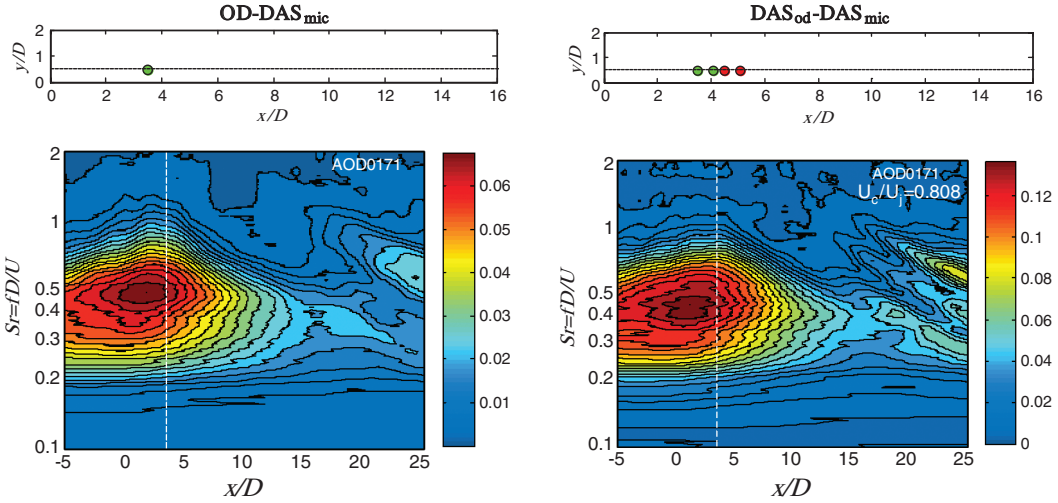

Fig. 15 Isocontours of coherence for OD-DAS$_{mic}$ and DAS$_{od}$-DAS$_{mic}$. Reference probe at $x/D = 3.5$ and $r/D = 0.48$ (lip line). Computed convective velocity $U_c = 0.81\ U_j$ was used in DAS$_{od}$ beamforming.

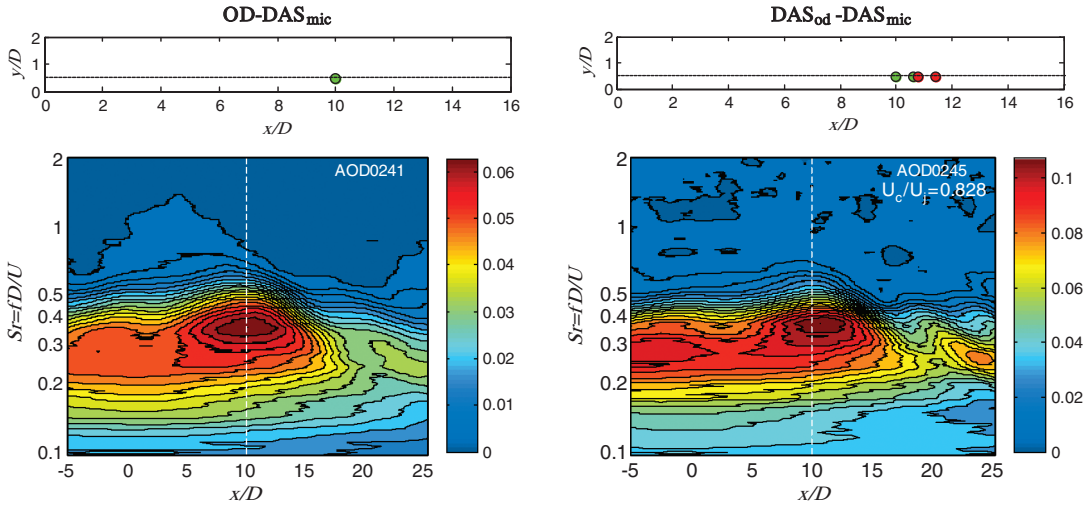

Fig. 16 Isocontours of coherence for OD-DAS$_{mic}$ and DAS$_{od}$-DAS$_{mic}$. Reference probe at $x/D = 10$ and $r/D = 0.48$ (lip line). Computed convective velocity $U_c = 0.83\ U_j$ was used in DAS$_{od}$ beamforming.

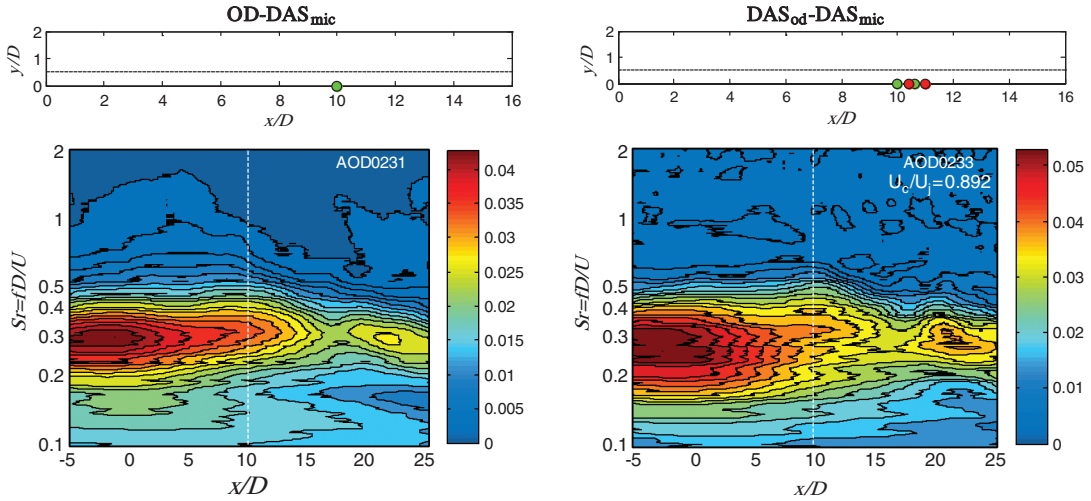

Fig. 17 Isocontours of coherence for OD-DAS$_{mic}$ and DAS$_{od}$-DAS$_{mic}$. Reference probe at $x/D = 10$ and $r/D = 0$ (centerline). Computed convective velocity $U_c = 0.89\ U_j$ was used in DAS$_{od}$ beamforming.

V. Conclusions

Simultaneous multipoint measurements in the flowfield and acoustic field of a Mach 1.75 cold-air jet with supersonic convection velocity have been conducted. A series of four OD probes were used for the flowfield measurements, and eight microphones arranged on a circular arc recorded the far-field pressure in the direction of peak emission. In addition, some of the OD probes were moved to the near acoustic field of the jet. The correlation methodology involves calculating the delay-and-sum beamformer outputs of the OD probes and microphones, then computing the coherence between the two outputs. The principal conclusions are as follows:

1) With the OD probes in the jet shear layer, there is a significant correlation, on the order of 0.1, between turbulence and far-field noise in the direction of peak emission.

2) As the OD probe moves transversely away from the jet, the coherence with the far-acoustic field first drops and then increases significantly to levels on the order of 0.3. The drop is associated with the probe moving into the hydrodynamic pressure field that does not radiate to the far field; the subsequent increase signifies the probe being located in the acoustic pressure field.

3) In the vicinity of the jet exit, the peak coherence between OD signal and microphone beamformer coincides with the physical location of the OD probe. However, as the shear layer thickens downstream, the peak coherence generally lags the probe location. It is believed that this is caused by the refraction of the acoustic rays by the mean velocity and speed-of-sound gradients. The effect is particularly severe when the OD probe is on the jet centerline beyond the end of the potential core. This underscores the need to include refraction effects in the calculation of the beamformer output of the microphone array.

4) Correlation of the beamformed OD signal, using the measured convection velocity of the turbulence, with the microphone beamformed output produces isocontours with the greatest fidelity and with significantly higher coherence levels than obtained with single OD to microphone correlations. This method thus promises to produce data that will be more useful in assisting the development of predictive models for the various noise generation mechanisms.

5) The increased coherence levels associated with the beamformed OD-microphone correlations indicates that the noise radiated in the peak noise radiation direction is associated with turbulence convecting at U_c, which is determined experimentally, and is coherent over a relatively large axial distance. This is additional strong evidence for the importance of the coherent large-scale turbulent structures in noise radiation from high-speed jets.

References

[1] McLaughlin, D. K., Morrison, G. L., and Troutt, T. R., "Experiments on the Instability Waves in a Supersonic Jet and Their Acoustic Radiation," *Journal of Fluid Mechanics*, Vol. 69, May 1975, pp. 73–85. doi:10.1017/S0022112075001322

[2] Troutt, T. R., and McLaughlin, D. K., "Experiments on the Flow and Acoustic Properties of a Moderate-Reynolds-Number Supersonic Jet," *Journal of Fluid Mechanics*, Vol. 116, Mar. 1982, pp. 123–156. doi:10.1017/S0022112082000408

[3] Morris, P. J., "Flow Characteristics of the Large-Scale Wavelike Structure of a Supersonic Round Jet," *Journal of Sound and Vibration*, Vol. 53, No. 2, 1977, pp. 223–244. doi:10.1016/0022-460X(77)90467-9

[4] Tam, C. K. W., "Directional Acoustic Radiation from a Supersonic Jet Generated by Shear Layer Instability," *Journal of Fluid Mechanics*, Vol. 46, Apr. 1971, pp. 757–768. doi:10.1017/S0022112071000831

[5] Tam, C. K. W., "Supersonic Jet Noise Generated by Large Scale Disturbances," *Journal of Sound and Vibration*, Vol. 38, No. 1, 1975, pp. 51–79. doi:10.1016/S0022-460X(75)80020-4

[6] Tam, C. K. W., and Morris, P. J., "The Radiation of Sound by the Instability Waves of a Compressible Plane Turbulent Shear Layer," *Journal of Fluid Mechanics*, Vol. 98, No. 2, 1980, pp. 349–381. doi:10.1017/S0022112080000195

[7] Panda, J., Seasholtz, R. G., and Elam, K. A., "Measurement of Correlation Between Flow Density and Velocity with Far Field Noise in High Speed Jets," AIAA Paper 2002-2485, Jan. 2002.

[8] Panda, J., and Seasholtz, R. G., "Experimental investigation of Density Fluctuations in High-Speed Jets and Correlation with Generated Noise," *Journal of Fluid Mechanics*, Vol. 450, Jan. 2002, pp. 97–130.

[9] Fisher, M. J., Harper-Bourne, M., and Glegg, S. A. L., "Jet Engine Source Location: The Polar Correlation Technique," *Journal of Sound and Vibration*, Vol. 51, No. 1, 1977, pp. 23–54. doi:10.1016/S0022-460X(77)80111-9

[10] Billingsley, J., and Kinns, R., "The Acoustic Telescope," *Journal of Sound and Vibration*, Vol. 48, No. 4, 1976, pp. 485–510. doi:10.1016/0022-460X(76)90552-6

[11] Humphreys, W. M., Brooks, T. F., Hunter, W. W., and Meadows, K. R., "Design and Use of Microphone Directional Arrays for Aeroacoustic Measurements," AIAA Paper 98-0471, Jan. 1998.

[12] Brooks, T. F., and Humphreys, W. M., "A Deconvolution Approach for the Mapping of Acoustic Sources (DAMAS) Determined from Phased Microphone Arrays," *Journal of Sound and Vibration*, Vol. 294, Nos. 4–5, pp. 856–879. doi:10.1016/j.jsv.2005.12.046, 2006.

[13] Lee, S. S., and Bridges, J., "Phased-Array Measurements of Single Flow Hot Jets," AIAA Paper 2005-2842, May 2005.

[14] Venkatesh, S. R., Polak, D. R., and Narayanan, S., "Beamforming Algorithm for Distributed Source Localization and its Application to Jet Noise," *AIAA Journal*, Vol. 41, No. 7, 2003, pp. 1238–1246. doi:10.2514/2.2092

[15] Papamoschou, D., "Imaging of Distributed Directional Noise Sources," AIAA Paper 2008-2885, May 2008.

[16] Bridges, J., "Effect of Heat on Space-Time Correlations in Jets," AIAA Paper 2006-2534, May 2006.

[17] Hileman, J. I., Thurow, B. S., Caraballo, E. J., and Samimy, M., "Large-Scale Structure Evolution and Sound Emission in High-Speed Jets:

Real-Time Visualization with Simultaneous Acoustic Measurements," *Journal of Fluid Mechanics*, Vol. 544, Dec. 2005, pp. 277–307. doi:10.1017/S002211200500666X

[18] Doty, M. J., and McLaughlin, D. K., "Two-Point Correlations of Density Gradient Fluctuations in High Speed Jets Using Optical Deflectometry," AIAA Paper 2002-0367, Jan. 2002.

[19] Doty, M. J., and McLaughlin, D. K., "Space-Time Correlation Measurements of High-Speed Axisymmetric Jets Using Optical Deflectometry," *Experiments in Fluids*, Vol. 38, No. 4, 2005, pp. 415–425. doi:10.1007/s00348-004-0920-1

[20] Petitjean, B., Viswanathan, K., McLaughlin, D. L., and Morris, P. J., "Space-Time Correlation Measurements in Subsonic and Supersonic Jets Using Optical Deflectometry," AIAA Paper 2007-3613, May 2007.

[21] Veltin, J., Day, B., and McLaughlin, D. K., "Correlation of Flow and Acoustic Field Measurements in High Speed Jets," AIAA Paper 2009-3211, May 2009.

[22] Kerherve, F., Jordan, P., Gervais, J. C., Valiere, J. C., and Braud, P., "Two-Point Laser Doppler Velocimetry Measurements in a Mach 1.2 Cold Supersonic Jet for Statistical Aeroacoustics Source Models," *Experiments in Fluids*, Vol. 37, No. 3, 2004, pp. 419–437.

[23] Seiner, J. M., McLaughlin, D. K., and Liu, C. H., "Supersonic Jet Noise Generated by Large-Scale Instabilities," NASA TP 2072, Sept. 1982.

[24] Morris, P. J., and Zaman, K., "Velocity Measurements in Jets with Application to Noise Source Modeling," *Journal of Sound and Vibration*, Vol. 329, No. 4, 2010, pp. 394–414. doi:10.1016/j.jsv.2009.09.024

[25] Day, B. J., "Turbulence Measurements in Supersonic Jets with Optical Deflectometry," M.S. Thesis, Pennsylvania State Univ., University Park, PA, May 2010.

[26] Davies, P. O. A. L., "Turbulence Structure in Free Shear Layers," *AIAA Journal*, Vol. 4, No. 11, 1966, pp. 1971–1978. doi:10.2514/3.3827

[27] Bogey, C., and Bailly, C., "An Analysis of the Correlations between the Turbulent Flow and the Sound Pressure Fields of Subsonic Jets," *Journal of Fluid Mechanics*, Vol. 583, July 2007, pp. 71–97. doi:10.1017/S002211200700612X

[28] Arndt, R. E. A., Long, D. F., and Glauser, M. N., "The Proper Orthogonal Decomposition of Pressure Fluctuations Surrounding a Turbulent Jet," *Journal of Fluid Mechanics*, Vol. 340, 1997, pp. 1–33. doi:10.1017/S0022112097005089

[29] Coiffet, F., Jordan, P., Delville, J., and Gervais, Y., "Coherent Structures in Subsonic Jets: A Quasi-Irrotational Source Mechanicsm?," *International Journal of Aeroacoustics*, Vol. 5, No. 1, 2006, pp. 1–24.

[30] Guitton, A., Jordan, P., Laurendau, E., and Delville, J., "Velocity Dependence on the Near Field of Subsonic Jets: Understanding the Associated Source Mechanisms," AIAA Paper 2007-3661, May 2007.

M. Glauser
Associate Editor